Companion blood cells control ovarian stem cell niche microenvironment and homeostasis

Véronique Van de bor, Geordie Zimniak, Lise Papone, Delphine Cerezo, Marilyne Malbouyres, Thomas Juan, Florence Ruggiero, Stéphane Noselli

Article

Cell Reports

Companion Blood Cells Control Ovarian Stem Cell Niche Microenvironment and Homeostasis

Graphical Abstract

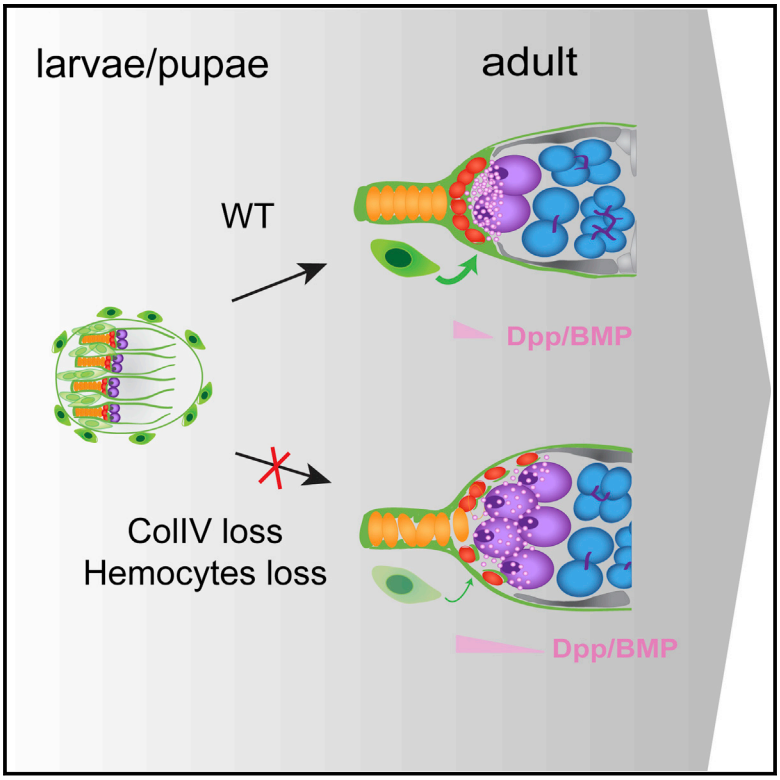

Authors

Véronique Van De Bor, Geordie Zimniak, Lise Papone, ..., Thomas Juan, Florence Ruggiero, Stéphane Noselli

Correspondence

vandebor@unice.fr (V.V.D.B.), noselli@unice.fr (S.N.)

In Brief

The ECM is important for stem cell niche development and function, but its origin is not well defined. Van de Bor et al. find that "companion" hemocytes associate with the *Drosophila* female gonad to secrete ColIIV present in the adult stem cell niche. Their results show that hemocyte-derived ColIIV is essential for stem cell niche organization and stem cell number.

Highlights

- "Companion" hemocytes associate with the female larval gonad
- Hemocytes produce functional ECM in the germline stem cell (GSC) niche
- Loss of hemocyte-derived ColIIV leads to abnormal stem cell niche with excess GSCs
- Hemocyte-derived ColIIV controls the extent of BMP signaling and niche homeostasis

Van De Bor et al., 2015, Cell Reports *13*, 546–560
October 20, 2015
http://dx.doi.org/10.1016/j.celrep.2015.09.008

OPEN ACCESS
CellPress

Cell Reports
Article

Companion Blood Cells Control Ovarian Stem Cell Niche Microenvironment and Homeostasis

Véronique Van De Bor,[1,2,3,*] Geordie Zimniak,[1,2,3] Lise Papone,[1,2,3] Delphine Cerezo,[1,2,3] Marilyne Malbouyres,[4] Thomas Juan,[1,2,3] Florence Ruggiero,[4] and Stéphane Noselli[1,2,3,*]
[1]University of Nice Sophia Antipolis, Institut de Biologie Valrose, iBV, 06108 Nice, France
[2]CNRS, Institut de Biologie Valrose, iBV, UMR 7277, 06108 Nice, France
[3]INSERM, Institut de Biologie Valrose, iBV, U1091, 06108 Nice, France
[4]Institut de Génomique Fonctionnelle de Lyon-ENS de Lyon, CNRS UMR 5242, INRA USC 1370, 46, allée d'Italie, 69364 Lyon Cedex 07, France
*Correspondence: vandebor@unice.fr (V.V.D.B.), noselli@unice.fr (S.N.)
http://dx.doi.org/10.1016/j.celrep.2015.09.008

SUMMARY

The extracellular matrix plays an essential role for stem cell differentiation and niche homeostasis. Yet, the origin and mechanism of assembly of the stem cell niche microenvironment remain poorly characterized. Here, we uncover an association between the niche and blood cells, leading to the formation of the *Drosophila* ovarian germline stem cell niche basement membrane. We identify a distinct pool of plasmatocytes tightly associated with the developing ovaries from larval stages onward. Expressing tagged collagen IV tissue specifically, we show that the germline stem cell niche basement membrane is produced by these "companion plasmatocytes" in the larval gonad and persists throughout adulthood, including the reproductive period. Eliminating companion plasmatocytes or specifically blocking their collagen IV expression during larval stages results in abnormal adult niches with excess stem cells, a phenotype due to aberrant BMP signaling. Thus, local interactions between the niche and blood cells during gonad development are essential for adult germline stem cell niche microenvironment assembly and homeostasis.

INTRODUCTION

Stem cells provide organs with plasticity and regenerative capabilities essential for normal development and aging. Defective stem cell function leads to a number of pathologies, including severe congenital disorders, neurodegenerative diseases, and cancer (Bateman et al., 2009; Kim et al., 2011; Wong et al., 2012; Yurchenco, 2011). An important aspect of stem cell biology is the organization into a functional niche, which provides a specialized 3D microenvironment sustaining stem cells through the control of their proliferation and pluripotent states (Schofield, 1978; Spradling et al., 2001). Therefore, understanding the molecular mechanisms governing stem cell niche development, structure, and homeostasis is of prime interest. The extracellular matrix (ECM) is an essential component of the niche (reviewed in Daley et al., 2008), whose alteration can affect stem cell maintenance, proliferation, and differentiation (Gattazzo et al., 2014; Guo and Wang, 2009; Lu et al., 2012; Ricard-Blum and Ruggiero, 2005; Tanimura et al., 2011; Watt and Huck, 2013). Although progress has been made in elucidating stem cell niche function, it remains unclear how exactly the niche microenvironment assembles during development and what are its components as well as their dynamics and functions in vivo.

Drosophila ovaries represent a valuable, genetically tractable model to investigate stem cell niche development in vivo. Adult ovaries are composed of approximately 20 ovarioles containing egg chambers surrounded by a thin muscular sheath (Hudson et al., 2008). These egg-producing units arise from two pools of stem cells: the somatic and the germline stem cells (GSCs), located in the germarium at the apex of the ovariole (Figure 1A). The GSC niche itself is made of a group of five to seven cap cells positioned at the tip of the germarium, contacting the terminal filament cells anteriorly and anchoring GSCs posteriorly through DE-cadherin-β-catenin-mediated adhesion (Song et al., 2002). Cap cells produce the decapentaplegic (Dpp)/BMP ligand to maintain the GSC pool (Chen and McKearin, 2003; Guo and Wang, 2009; Harris and Ashe, 2011; Losick et al., 2011; Xie and Spradling, 1998).

The ECM in *Drosophila* essentially consists of basement membrane (BM), aka basal lamina (Fessler and Fessler, 1989). BMs provide mechanical stability to organs and are essential for migration, survival, proliferation, and differentiation (Khoshnoodi et al., 2008; LeBleu et al., 2007; Yurchenco, 2011). They are made of self-assembled collagen IV (ColIV) and laminin networks essential for BM stability. Nidogen/entactin and perlecan crosslink the laminin and ColIV networks, increasing their stability and controlling the structural integrity of the overall membrane. *Drosophila* ColIV consists of two α chains, α-1 (Cg25c) and α-2 (Vkg), which form heterotrimers (Blumberg et al., 1988; Lunstrum et al., 1988) that are post-translationally modified by lysyl and prolyl hydroxylases enzymes, ultimately forming a functional BM (Bunt et al., 2010; Lerner et al., 2013; Pastor-Pareja and Xu, 2011). In adult ovaries, somatic follicular cells produce

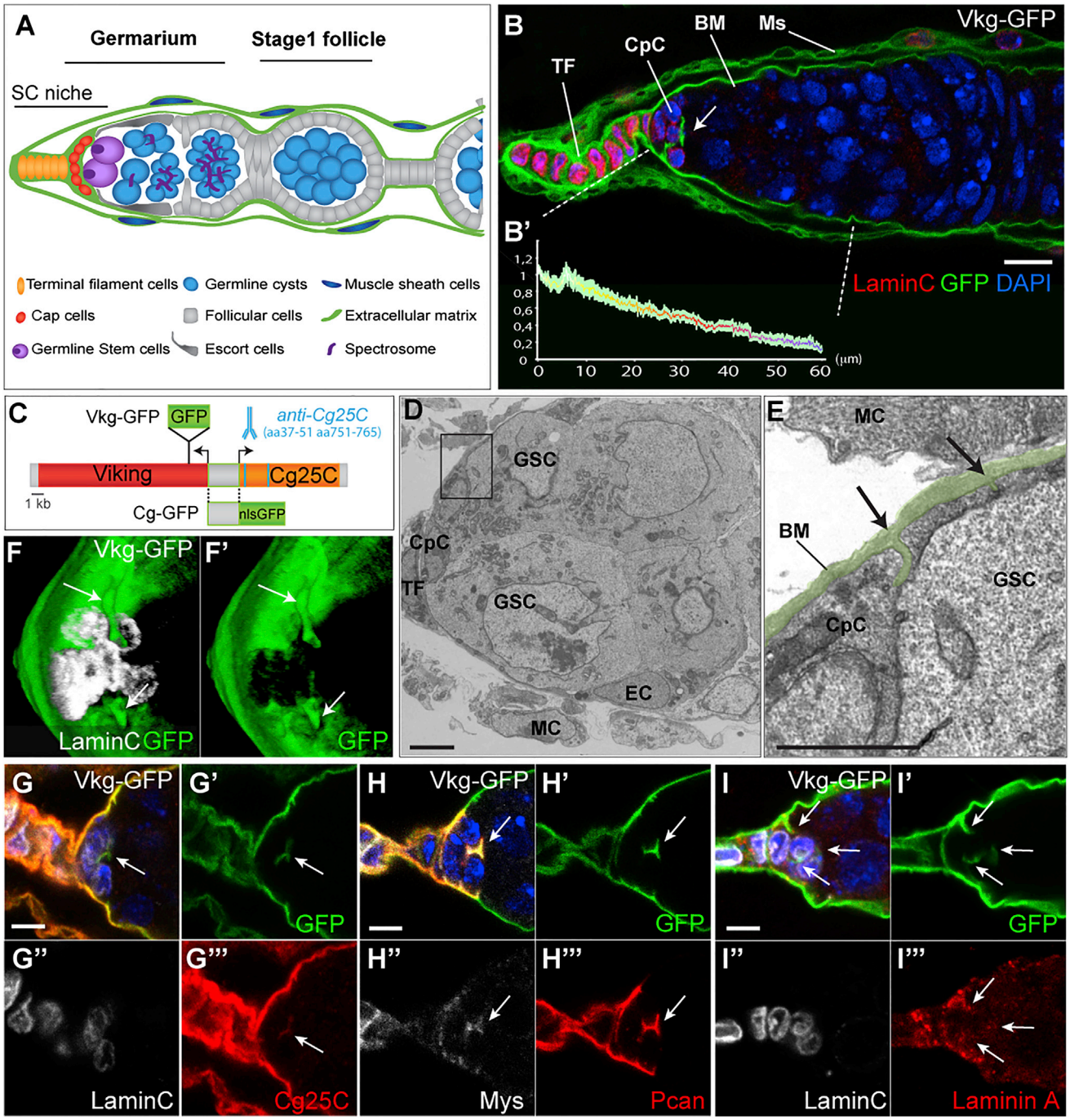

Figure 1. Germline Stem Cell Niche BM Organization

(A) Schematic of the earliest stages of oogenesis. (BM, basement membrane; CpC, cap cells; EC, escort cell; GSC, germline stem cell; MC, muscular sheath cell; Ms, muscular sheath; TF, terminal filament cell).

(B) A Vkg-GFP (green) germarium stained for DNA (DAPI; blue) and LaminC (red) to reveal the TF (strong red signal) and the CpC (weaker signal). Vkg is present in the BM around the MC, the germarium, and as an interstitial aggregate around the CpC (arrow). (B') Quantification of GFP signal from 30 different germaria is shown.

(C) Schematic of the ColIV locus and the tools used in this study. The Vkg-GFP protein trap line is shown. The anti-Cg25C antibody raised against two peptides (aas 37–51 and aas751–765 blue bars) is shown. The Cg-GFP reporter line shows fusion of the promoter region shared by Viking and Cg25C with an nls-GFP sequence.

(D) Transmission electron microscopy showing germarium ultrastructure. The scale bars represent 1 μm.

(E) High magnification of the box in (D). Arrows show two invaginations of the BM highlighted in green.

(legend continued on next page)

ColIV, which is basally assembled into an egg chamber BM network through a Crag/Rab10/PIs-dependent mechanism (Denef et al., 2008; Devergne et al., 2014; Lerner et al., 2013; Medioni and Noselli, 2005). This specific ColIV plays an essential role in the establishment and maintenance of follicle cell polarity and in promoting egg elongation (Haigo and Bilder, 2011; Horne-Badovinac et al., 2012). Although BM material also covers the germarium, its exact role remains unknown. A first hint for a possible role of BM in *Drosophila* stem cell niche function comes from *vkg* hypomorphic mutants in which an excess of GSCs is observed (Wang et al., 2008). In addition, recent work showed that Dpp binds to ColIV N-terminal region (Wang et al., 2008). Therefore, studying the origin, dynamics, architecture, and role of the *Drosophila* stem cell niche ECM should reveal mechanisms important for GSCs homeostasis.

Here, we characterized the genesis and role of the BM during GSC niche development. Analysis of the composition and organization of the BM showed that the GSC niche contains both regular and interstitial basal lamina material important in sustaining stem cells. We revealed that the GSC niche BMs have a non-autonomous origin and are contributed by tightly associated companion blood cells, called hereafter ''ovarian hemocytes''. This association is developmentally regulated. The ovarian hemocytes associate with the GSC niche in the larval gonad and build a hemocyte-derived BM that is highly stable from larval to adult stages. Disrupting the larval BM induces dramatic changes in adult GSC niche organization and homeostasis, leading to supernumerary stem cells, a phenotype that is due to excess diffusion of the Dpp/BMP ligand. Altogether, our results identify a role for blood cells in making a permanent BM, which shapes the adult GSC niche and controls its homeostasis. These findings allow proposing a general model of BM assembly with emerging properties.

RESULTS

Composition and Structure of the Ovarian GSC Niche BM

To characterize the ovarian GSC niche BM, we first analyzed ColIV expression in the germarium using a Vkg-GFP fusion protein (Medioni and Noselli, 2005; Morin et al., 2001) and specific anti-Cg25c antibodies (Figures 1B, 1C, and S1A–S1F; see Experimental Procedures). Vkg and Cg25c showed perfect co-localization in the germarium as well as in other ovarian tissues and stages (Figure 1G; not shown). Both proteins are detected as two extracellular BM layers lining the muscular sheath and the germarium (Figures 1A and 1B). Signal quantification of Vkg-GFP revealed an anterior-posterior gradient in the germarium, with a higher intensity observed around the cap cells (Figure 1B'). Interestingly, Vkg and Cg25c were also detected at the interface between cap cells and GSCs, thus forming an interstitial matrix (Figures 1B and 1G–1G'''). 3D image reconstruction revealed that this interstitial ColIV is made of rough and irregular structures embedding the cap cells, an organization contrasting with typical epithelial BM layers (Figures 1F and 1F'; Movie S1). Analyzing matrix ultrastructure using transmission electron microscopy (TEM) confirmed that the BM surrounding the germarium forms extensions filling the extracellular space; in addition, it revealed that the BM thickens around the GSC niche, consistent with Vkg-GFP protein concentration profiles (Figures 1B', 1D, and 1E). To further characterize the composition of the GSC niche ECM, we sought out the different components commonly found in BMs. Results show that perlecan, the laminin A subunit, as well as the integrin βPS subunit myospheroid are also present in the regular and interstitial matrices surrounding the cap cells (Figures 1H–1I''' and S1G–S1J). Noticeably, perlecan is specifically enriched around and within the niche (Figure 1H), revealing a sharp ECM boundary between the GSC niche and more-posterior regions of the germarium. Altogether, these results show the existence of a specialized BM around the ovarian GSC niche, which extends inside the niche, forming an interstitial matrix.

Non-autonomous Origin of GSC Niche ColIV

In order to assess the origin of the ovarian niche BM, we first identified cells expressing the ColIV genes using the transcription reporter line Cg-GFP. Cg-GFP drives nuclear-GFP expression under the control of regulatory sequences common to the *vkg* and *cg25c* genes, which are organized head to head in the genome (Sorrentino et al., 2007; see Figure 1C). Cg-GFP shows expression in the fat body located underneath the abdomen and surrounding the ovaries (Figure 2A) as well as in all follicle cells starting from stage 6 egg chambers (Figure 2B). However, in the germarium, no Cg-GFP expression was detected in either somatic or germinal cells, suggesting that germarium ColIV is not synthesized by this tissue. Intriguingly, we observed a few Cg-GFP-positive cells outside the germarium and located in between the ovariole and the muscular sheath (Figure 2B). To confirm these observations, we performed in situ hybridization for *vkg* and *cg25c* mRNAs. We found that both transcripts are expressed in abdominal fat cells (Figures 2C and 2E) and in all follicular cells from stage 1 follicles onward (Figures 2D, 2F, and 2G; the difference between Cg-GFP pattern and in situ hybridization may reflect delay in Cg-GFP expression or in ColIV translation). Consistent with the Cg-GFP pattern (Figure 2B), we did not detect any ColIV transcripts in cells within the niche (Figures 2D, 2F, and 2G), although it should be noted that germarium mRNAs are difficult to detect by in situ hybridization. Finally, intracellular secretory vesicles, which are clearly visible in follicle cells (Figures S2G and S2H), expressing ColIV, were not observed in germarium (cap or escort cells; GSCs; Figures S2C, S2D, and S2D') except when UAS-GFP-Vkg was ectopically expressed (Figures S2E and S2F).

Interestingly, in situ hybridization shows that the intriguing Cg-GFP cells located outside the germarium strongly express both *vkg* and *cg25c* transcripts (Figures 2F, 2G, 2I, and 2J). Thus, the Cg-GFP reporter line, in situ hybridization, and intracellular

(F and F') A Vkg-GFP germarium 3D reconstruction revealing two deep Vkg-GFP invaginations (arrows) around CpC (stained with Lamin C [white]).
(G–I''') Vkg-GFP germline stem cell niches stained for different ECM markers. (G) LaminC (white) and Cg25C (red), (H) Perlecan (Pcan) (red) and Myospheroid (Mys) (white), and (I) LaminC (white) and Laminin A (red) are shown; scale bars, 6.5 μm.
See also Figure S1 and Movie S1.

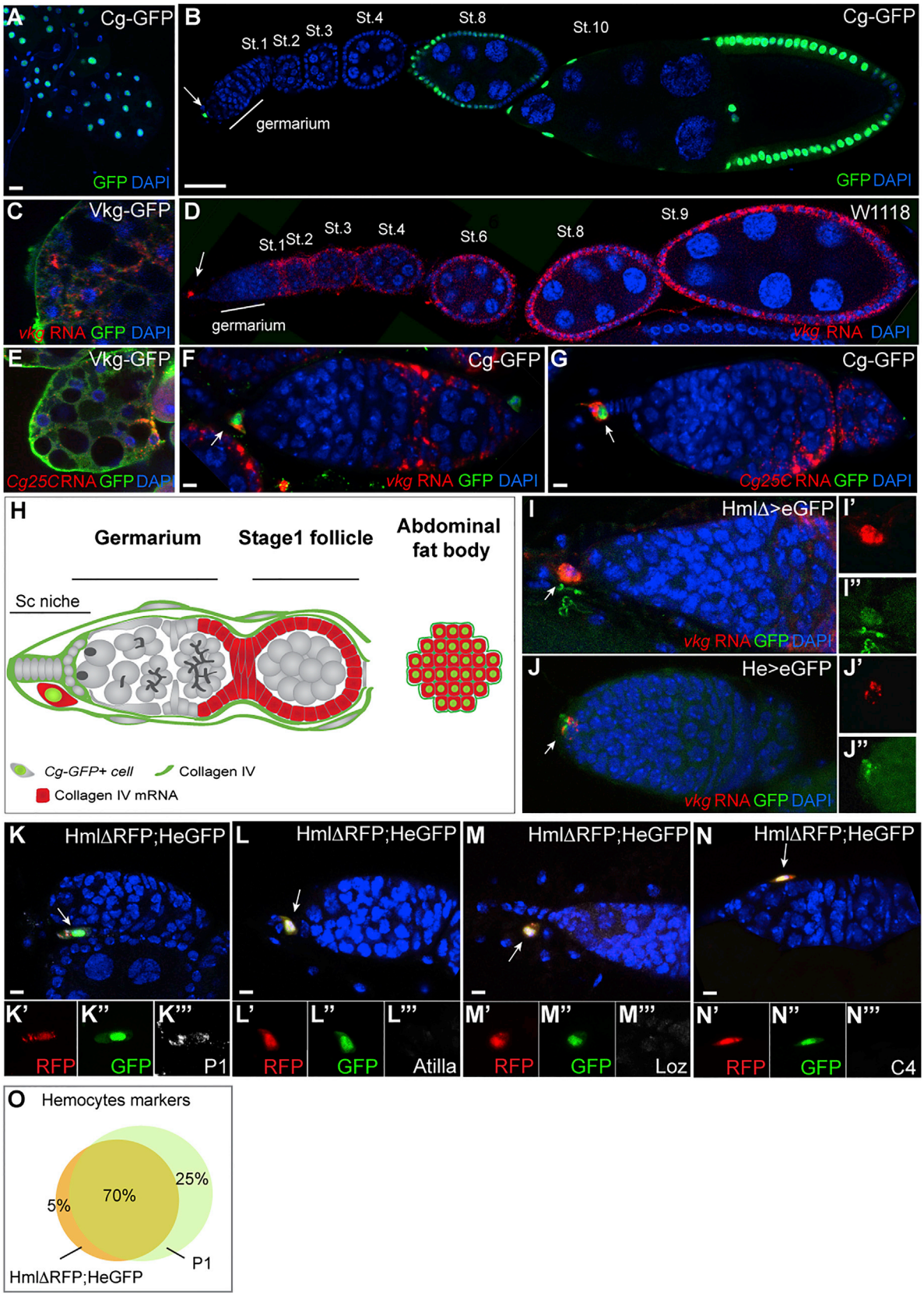

(legend on next page)

Vkg-GFP vesicles reveal ColIV expression in the abdominal fat body, the follicular cells, and in a few still unidentified germarium-associated cells. Importantly, these analyses suggested the absence of ColIV expression in the cells present within the GSC niche itself, indicating that both regular and interstitial ColIV surrounding the GSC stem cell niche is not provided by the germarium but instead has a non-autonomous origin.

Hemocytes Are Associated with the Ovarian GSC Niche

The identification of germarium-associated ColIV-expressing cells is puzzling and raises the question of their identity and role. Their shape, size, and the fact that they are Cg-GFP-positive suggest they could correspond to blood cells, aka hemocytes. Three types of hemocytes have been characterized in flies (Jung et al., 2005; Lanot et al., 2001; Tepass et al., 1994): (1) plasmatocytes, which are small spherical cells responsible for phagocytosis. At embryogenesis, they express different ECM components (including ColIV) that assemble BM around organs; (2) lamellocytes, which are large flat cells involved in encapsulation differentiating upon parasitic infection; and (3) crystal cells, which are involved in pathogen melanization. The different types of blood cells can be identified using specific markers. All three classes of hemocytes express the Hemese (He) marker early during development (Kurucz et al., 2003), whereas a majority of plasmatocytes and crystal cells express Vkg, Cg25c, Cg-GFP, and the Von-Willebrand-like factor hemolectin (Hml). Specific differentiation markers are also expressed in each lineage: NimrodC1 (P1) in plasmatocytes; Atilla in lamellocytes and lozenge (lz); and C4 in crystal cells (Lebestky et al., 2000; Wood and Jacinto, 2007). To test for the presence of ColIV-producing hemocytes in adult ovaries, we performed in situ hybridization for *vkg* or *cg25c* in *HmlΔ-Gal4 > GFP* and *He-Gal4>GFP* reporter lines. Interestingly, results show that cells expressing ColIV in the germarium are also positive for the Hml and He markers (Figures 2I and 2J), demonstrating that adult ovaries contain hemocytes, hereafter referred to as ''ovarian hemocytes''. To further characterize these hemocytes, we used specific blood cell lineage markers along with double labeling for Hml and He (*HmlΔRFP*; *He-Gal4 > GFP* flies). This revealed that ovarian hemocytes express the plasmatocyte marker P1, but not Atilla (lamellocyte marker) nor Lz or C4 (crystal cell marker; Figures 2K–2N). We conclude that ovarian hemocytes belong to the plasmatocyte subtype.

Detailed analysis showed that, whereas the majority of *HmlΔRFP*; *He-Gal4 > GFP* hemocytes express the P1 marker, a small proportion do not (5%); in addition, some P1-positive cells do not express Hml or He (25%), suggesting that ovarian plasmatocytes are present in at least three differentiation stages (Figure 2O). The proliferative state of these cell populations was analyzed by anti-phosphohistone H3 (PH3) staining; no mitosis figure was detectable (0/150), suggesting a very low proliferation rate for these cells, consistent with previous studies performed on adult hemocytes (data not shown; Lanot et al., 2001).

Altogether, these results reveal the presence of ColIV-positive hemocytes of the plasmatocyte type tightly associated with the ColIV-negative GSC niche, thus raising the question of the role of ovarian plasmatocytes in both ColIV production and GSC niche function.

Ovarian Hemocytes Produce GSC Niche ColIV

ColIV is thought to be provided to organs in a systemic way through the hemolymph. However, our data suggest that GSC stem cell niche ColIV may in fact be produced from specific ovarian plasmatocytes. To control Vkg and Cg25c tissue-specific expression using the Gal4-UAS system and thus trace the origin of the ColIV found around the niche unambiguously, we engineered GFP-tagged forms of the large secreted molecules Vkg and Cg25c α chains (hereafter referred to as inGFP-Vkg and inGFP-Cg25C; the ''in'' prefix refers to ''inducible''; see Experimental Procedures). The GFP tag was inserted inside the coding region, as in the widely used Vkg-GFP protein-trap line (see Experimental Procedures). Importantly, the *UAS-GFP-Vkg* and *UAS-GFP-Cg25c* constructs did not lead to any dominant phenotype when overexpressed and our genetic data show that *UAS-GFP-Vkg* can rescue the lethality of the vkg^{k00236} mutant (data not shown). Finally, expression of the two proteins under the control of the *Cg-Gal4* driver (which is made of the ColIV regulatory region fused to *Gal4*; Asha et al., 2003; and recapitulates ColIV expression profile) show a BM pattern that is indistinguishable from the endogenous one (tested with Vkg-GFP and antibody labeling; Figure 3A; data not shown). Altogether, these data indicate that the inGFP-Vkg and inGFP-Cg25C proteins are functional and can integrate the BM without being deleterious to the organism, thus constituting valuable tools.

To analyze ColIV cell autonomy and range, inGFP-Vkg and inGFP-Cg25C were expressed using a range of tissue-specific

Figure 2. ColIV Expression Pattern in Ovaries

(A) Cg-GFP adult abdominal fat body.

(B) Cg-GFP ovariole. No signal is detected in the stem cell niche and germarium. Signal is detected in follicular cells from stage 6 egg chambers and in cells scattered between the ovariole and the muscular sheath (arrow). The scale bar represents 50 μm.

(C–G) In situ hybridization (red) against *vkg* (C, D, and F) and *cg25C* mRNAs (E and G) on Vkg-GFP abdominal fat body (C and E) or Cg-GFP germaria (F and G). The Cg-GFP cells associated with the germarium express both *vkg* (F) and *cg25c* mRNAs (G). (D) Composite image from an ovariole is shown; middle cross-section of each egg chamber was assembled. The scale bar represents 5 μm.

(H) ColIV expression from (A)–(G).

(I and J) In situ hybridization against *vkg* mRNA (red) combined with anti-GFP labeling (green) of HmlΔ > eGFP (H) or He > eGFP (I) germaria. Cells associated with the germarium express hemocyte markers (arrows). (I', I'', J', and J'') Higher magnification of the cells pointed in (I) and (J) is shown. The scale bar represents 5 μm.

(K–N''') *HmlΔ-RFP*; *He-Gal4 > GFP* germarium stained for plasmatocyte marker P1 (K–K'''), lamellocyte marker Atilla (L–L'''), and crystal cells marker Lozenge (Loz) (M–M''') and C4 (N–N'''). The scale bar represents 5 μm.

(O) Percentage of HmlΔ-RFP; He > GFP or P1-positive adult ovarian hemocytes.

See also Figure S2.

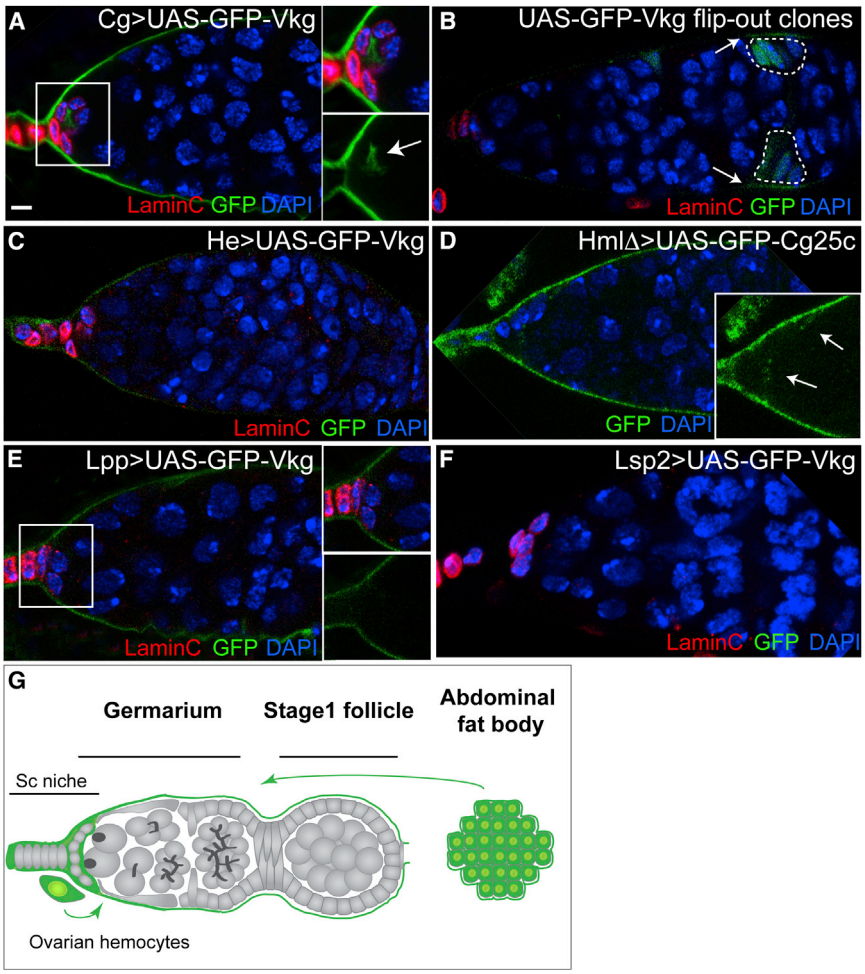

Figure 3. Origin of Germarium CollV

(A) Cg > UAS-GFP-Vkg germarium stained for LaminC (cap cells, red) and DAPI (DNA, blue). GFP is detected in the BM around the germarium and invaginations around the cap cells (arrow in close-up box).

(B) inGFP-Vkg flip-out clones in stage 1 follicle, stained for DNA (DAPI, blue). GFP is detected only at the basal side of the expressing cells (arrows).

(C–F) inGFP-Vkg (green) driven by specific Gal4 drivers. Germaria stained for LaminC (cap cells, red) and DNA (DAPI, blue) are shown. (C) He > UAS-GFP-Vkg germarium shows GFP signal in the BM around the germarium. (D) HmlΔ > UAS-GFP-Cg25C germarium shows GFP signal in the BM around the germarium and in the germline stem cell niche (arrows). (E) Lpp > UAS-GFP-Vkg germarium shows GFP in the BM around the germarium. (F) Lsp2 > UAS-GFP-Vkg germarium shows no GFP. The scale bar represents 5 μm.

(G) Contribution of ovarian hemocytes and abdominal fat body to the deposition of CollV in the germarium.

See also Figure S3.

Gal4 lines. Targeted expression of inGFP-Vkg in a subset of follicular cells (flip-out clones, *c306-Gal4*, *Upd-Gal4*, or *Slbo-Gal4*) led to cell-autonomous formation of GFP-tagged BM, i.e., specifically contacting the producing cells (Figures 3B, S3E, and S3F; data not shown). Therefore, CollV secreted by the follicular epithelium does not contribute to CollV deposition within the niche. inGFP-Vkg expression driven in the larval and adult fat body (*Lpp-Gal4*) led to non-autonomous GFP deposition around the germarium (Figure 3E) and the rest of the ovariole including the muscular sheath (Figures S3A–S3D). To determine when fat cells contribute to this germarium CollV, we drove expression using the *Lsp2-Gal4* driver, which is specific of the larval fat body. Interestingly, we found no GFP signal in the BM around the germarium using the *Lsp2-Gal4* driver (Figure 3F), indicating that adult fat cells, but not larval fat cells, contribute to germarium CollV.

Strikingly, expression of inGFP-Vkg or inGFP-Cg25C using hemocyte-specific drivers (*He-Gal4* or *HmlΔ-Gal4*) led to strong accumulation of GFP in both regular and interstitial BMs present around and within the GSC stem cell niche, respectively (Figures 3C and 3D). Altogether, these results reveal that adult fat cells and ovarian hemocytes, but neither follicular cells nor CollV-negative germaria cells, contribute to the formation of the GSC niche microenvironment (Figure 3G).

Ovarian Hemocytes Are of Larval Origin and Associate with the Larval Gonad

Our data show that ovarian hemocytes associate with adult germaria and contribute to the formation of the GSC niche ECM. However, it is unclear when this association first takes place and when CollV is first deposited in the niche. To address the first question, we analyzed hemocyte-ovary association during female gonad development from larval-to-adult stages. In flies, blood cells have two distinct origins: the embryonic procephalic mesoderm and the larval lymph gland (Grigorian et al., 2011; Holz et al., 2003; Krzemien et al., 2010; Lanot et al., 2001; Tepass et al., 1994). Embryonic hemocytes (EH) persist throughout metamorphosis and are still detectable in the adult fly in hematopoietic pockets, forming sessile clusters (Gold and Brückner, 2014; Holz et al., 2003; Lanot et al., 2001; Makhijani et al., 2011; Makhijani and Brückner, 2012). Lymph gland hemocytes (LGHs) differentiate at the end of the third larval instar and enter the circulation at the white pupal stage upon lymph gland disaggregation. Because neither pupal nor adult hematopoietic organs have been identified so far, niche-associated ovarian hemocytes should consist of a mixture of EH and LGH (Holz et al., 2003). In order to better characterize the origin of hemocytes, we combined *HmlΔ–Gal4* with *TubGal80ts* to perform cell-lineage-tracing experiments (Figures 4A and 4A') while controlling the onset (t = 0) of tracing at different developmental periods (G-trace technique; Evans et al., 2009; see Experimental Procedures). GFP-marked hemocytes could be detected in adult ovaries when GFP expression was induced after 96 hr when the LGHs have not yet disseminated, suggesting an embryonic origin. The fact that we did not observe marking prior to 96 hr

could be due to a lower efficiency of the G-trace technique in early L1/L2 stages. To determine whether LGH can also contribute ovarian hemocytes, G-trace experiments using the LGH-specific Gal4 driver (Dot-Gal4) were performed, leading to GFP-marked ovarian hemocytes (Figure 4A''). Together, these results suggest a mixed origin for ovarian hemocytes.

We next studied the dynamics of hemocyte-niche association by following the number (Figure 4B) and distribution (Figures 4C–4G) of hemocytes at different developmental times. For this purpose, we used *HmlΔ-RFP*, *He-GFP*, and *Cg-GFP* strains. In these flies, hemocytes were found around the female gonad from the white pupal stage to 47 hr APF (after puparium formation) (Figures 4C and 4C'). Most interestingly, hemocytes were also found inside the gonad in contact with the terminal filament cells (Figures 4D and 4D'). The number of He-positive cells inside and outside gradually increased, reaching a maximum at 18 hr APF (Figures 4B and 4E–4E'') and then progressively decreased during later pupal and adult stages (Figures 4B, 4F, and 4G). Therefore, larval hemocytes associate dynamically with the gonad during pupariation (Figure 4H), suggesting that they provide ColIV to the GSC stem cell niche from these early stages.

Ovarian Hemocytes Provide Germarium ColIV at the Larval Stage

To determine exactly when ColIV becomes initially deposited in the ovary and when hemocytes start to produce niche ECM, we examined ColIV deposition in the female larval gonad. At the early larval stage, Vkg-GFP strongly accumulates in the BM surrounding the gonad from first instar larval stages onward (Figures 5A–5E). Interestingly, Vkg-GFP also accumulates inside the gonad starting at the second instar. Later on, at the white pupal stage, GSC niches have started to differentiate, showing anterior-posterior organization of the GSC niche with anterior stacked terminal filament (TF) cells connected to approximately seven cap cells (Sahut-Barnola et al., 1995). At this stage, intragonadal Vkg-GFP is strong and envelops each TF (Figures 5D and 5D'), with this network expanding across the germarium at 18 hr APF along with gonad elongation (Figures 5E and 5E'). At 47 hr APF, the BM surrounding the gonad is completely disaggregated and each germarium is clearly individualized and outlined by a ColIV membrane (Figures 5F and 5F'). Strikingly, when inGFP-Vkg is specifically expressed in the hemocytes using *He-Gal4* or *HmlΔ-Gal*, we found a similar ColIV pattern of deposition around the germarium and only faintly around the gonad (Figures 5G and 5H). Therefore, GSC niche ColIV originating from the larval hemocytes is assembled in the larval gonad during niche differentiation.

Larval GSC Niche ColIV Is Stable and Persists throughout Adult Stage

Although hemocytes synthesize ColIV during early gonadal development, it remains unclear whether this early BM is stable enough to contribute to adult stem cell niches. That GSC niche ColIV could mainly be deposited prior to adult life is supported by the fact that the number of hemocytes is at its highest level during larval stages and rapidly decreases as development goes on (see above; Figure 4B).

To assess the stability of ColIV in the germarium, we performed pulse chase experiments using the Gal4-Gal80ts system. Forty-eight-hour pulses of inGFP-ColIV expression were induced throughout fly development (day 0 to day 10) and the presence of GFP in the adult GSC niche assessed. Strikingly, pulsed expression of inGFP-Vkg between 96 hr and 144 hr of development is sufficient to observe ColIV accumulation in both the regular and interstitial adult GSC niche BM (Figures 6A and 6B). Note that this ColIV accumulation is still visible in 60-day-old flies. In contrast, induction of inGFP-Vkg expression out of this time window led to no clear accumulation in adult niches. Altogether, these results indicate that the hemocyte-derived GSC niche BM is assembled at the larval stage and from then onward the niche BM is extremely stable and perdures throughout the adult reproductive life.

Hemocyte-Derived ColIV Regulates Niche Organization and GSC Number

The complex, developmentally regulated process leading to the assembly of a stable BM from larval hemocytes suggests that BM plays an important role in GSC niche homeostasis. To test this hypothesis, Vkg expression was silenced in the hemocytes using the hemocyte-specific *HmlΔ-Gal4* line. Vkg-GFP from both the regular and interstitial BM was significantly reduced in germaria from *HmlΔ-Gal4 > Vkg^{RNAi}* flies (Figures 6C–6E). Interestingly, even an incomplete reduction of hemocyte-derived Vkg led to a strong disorganization of the GSC niche: TF cells, which are generally staked outside the germarium, were found within the germarium in 20% of ovarioles (n = 17; Figure 6D); the cap cells, whose number was not changed, were found dispersed within the germarium instead of being clustered at its extremity in 50% of samples (Figure 6D); and cap cells detached from the TF cells in 30% of cases, a phenotype that was never observed in the control (n = 12; Figures 6C and 6D). Because the organization of the GSC niche was affected, we next analyzed GSC development. GSCs can be identified based on their spherical α spectrin-rich spectrosome and the lack of the Bag of Marble (BAM) differentiation factor. Interestingly, silencing hemocyte-derived *vkg* or *cg25c* induced a significant increase in GSCs number compared to the control (Figures 6F–6H). The phenotype of single-gene knockdown could be enhanced by combining both *vkg* and *cg25c* RNAis (Figure 6H). In all conditions tested, GSCs are generally located close to the cap cells. These results are consistent with previous work showing an increased number of GSCs in *vkg* hypomorphic mutants (Wang et al., 2008). Alternatively, preventing normal ColIV post-translational modification through prolyl-hydroxylase enzyme PH4αEFB silencing or eliminating hemocytes through induction of the pro-apoptotic gene *reaper* induced a similar phenotype (Figures 6H and S4B). Finally, knocking down *vkg* or *cg25c* in the fat body (using Lpp-Gal4) did not affect the number of GSCs, showing that the GSC phenotype is hemocyte specific. Of note, loss of ColIV neither affects the ability of the stem cells to produce functional cystoblasts nor does it affect egg chamber morphology (data not shown). Altogether, these results show that GSC niche ColIV originating from larval/pupal hemocytes plays a specific and essential role in niche organization and in the regulation of the number of GSCs, possibly through

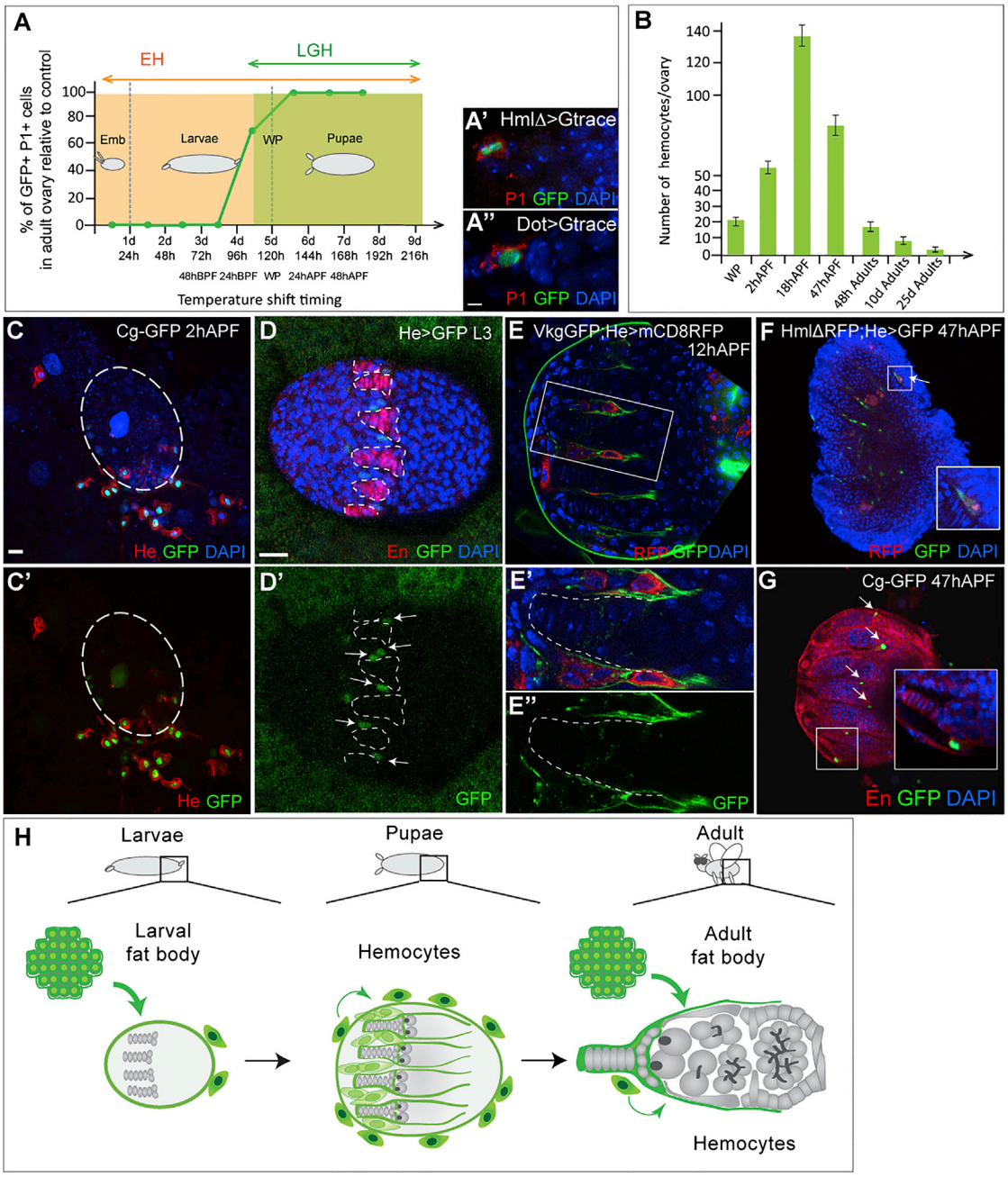

Figure 4. Hemocyte Associate with the Germline Stem Cell Niche in the Larval Gonad

(A) Graph showing the hemocyte lineage-tracing experiment. Results are represented as the relative % of GFP and P1-positive cells in adult ovaries compared to the control. GFP hemocytes are found in adult ovaries when GFP expression is induced after 84 hr of development. EH, embryonic hemocytes; LGH, lymph gland hemocytes. (A' and A'') G-trace experiments using *HmlΔ-Gal4* (A') or *Dot-Gal4* (A'') are shown. The scale bar represents 5 μm.

(B) Number of hemocytes per ovary in the He-GFP line.

(C and C') Cg-GFP gonad (2 hr after puparium formation [APF]) stained for the hemocyte marker Hemese (He, red) and DNA (DAPI, blue). The dashed lines highlight the shape of the gonad, with its anterior pole at the top and the posterior pole at the bottom. A group of Cg-GFP- and He-positive hemocytes surrounds the posterior side of the gonad.

(D and D') He > GFP third instar larval gonad stained for Engrailed (En, red; TF, dashed lines) and DNA (DAPI, blue). He-expressing cells are detected in between each developing TF (arrows in D').

(E) Vkg-GFP; He > mCD8RFP gonad (12 hr APF) stained for DNA (DAPI, blue). The scale bar represents 20 μm. (E' and E'') High magnification of the box in (E) showing He > mCD8RFP-positive cells surrounding the developing germaria (dashed lines).

(legend continued on next page)

different mechanisms, given that the frequency of phenotypes is not the same.

We have shown that the GSC niche BM is stably assembled at larval stages. To further test whether larval BM is specifically important for niche homeostasis, we silenced ColIV expression in hemocytes at different developmental times using the Gal4-Gal80ts system, as described above (Figures 6B and 6I). Hemocyte-derived ColIV was silenced by two different means: through expression of *Vkg-RNAi* or ablation of the hemocytes themselves. In both cases, we found a significant increase in GSCs when ColIV expression was abolished between 96 hr and 192 hr of development (Figure 6I). Therefore, the assembly of a stable GSC niche microenvironment occurring during larval development is essential for adult GSC niche homeostasis.

Hemocyte-Derived ColIV Controls Dpp Signaling and GSC Niche Homeostasis

The number of GSCs has been shown to be controlled by the Dpp/BMP-signaling pathway (reviewed in Harris and Ashe, 2011). Interestingly, Dpp has been reported to directly bind to Vkg C-terminal domain with Vkg enhancing Dpp signaling in the embryo (Wang et al., 2008). Furthermore, ectopic expression of Dpp leads to excess GSCs, indicating that Dpp positively controls GSC number in the germarium. Our genetic ablation of hemocyte-derived ColIV and *vkg* hypomorphic mutant phenotypes (Wang et al., 2008; data not shown) show a similar increase in GSCs, suggesting that *vkg* is a negative regulator in this process. To determine whether hemocyte-derived ColIV regulates the number of GSCs in a Dpp-dependent manner, we analyzed Dpp-signaling activity in *vkg*-deprived germaria using the Dad-lacZ reporter line (Casanueva and Ferguson, 2004; Song et al., 2004). Interestingly, affecting GSC niche ColIV through specific hemocyte-Vkg depletion led to an increased number of Dad-lacZ GSCs compared to the control; however, Dad-lacZ intensity remained equivalent to the control (Figures 7A–7D). These results suggest that perturbing the GSC niche BM leads to a broader diffusion of Dpp across the germanium. In this view, we hypothesized that decreasing the level of Dpp in Vkg-deprived germaria should rescue the increased GSC phenotype. Consistently, the average number of GSCs was back to normal in flies mutant for both *vkg* and *dpp* (Figures 7E–7G). Altogether, these results demonstrate that hemocyte-derived ColIV controls GSC number and niche homeostasis by restricting Dpp signaling (Figure 7H).

DISCUSSION

Designing tools to trace ColIV deposition in vivo allowed us to determine the spatial and temporal origin of the ECM present in the ovarian GSC niche. This approach revealed an association between the niche and blood cells, leading to the synthesis of a dedicated BM essential for GSC niche homeostasis. In this process, larval hemocytes build the future niche microenvironment, which is firmly maintained in adults and is essential for controlling BMP signaling and stem cell number. These results provide insights into the origin and dynamics of the GSC niche microenvironment, suggesting a general model for BM assembly and function during development.

Ovarian Hemocytes Are Essential for Adult GSC Niche Microenvironment, Organization, and Homeostasis

Our analysis of germaria BM composition and structure revealed two types of morphologically distinct matrices: (1) a regular one resembling the follicle cells BM, which lines the whole germarium and is characterized by a smooth appearance at the ultrastructural level and (2) a thicker and irregular BM filling the interstices between cap and stem cells. The structure of the interstitial matrix suggests it provides a net-like scaffold, maintaining cap and stem cell association. In support of this view, we found that reducing the level of ColIV leads to disorganized niches with cells losing their tight clustering and becoming dispersed. In addition to having a specific interstitial ECM, the GSC niche BM contains specific components like perlecan, whose pattern of accumulation shows a sharp boundary at the interface between the GSC niche and more-posterior structures. Particularities in GSC niche BM composition and appearance are suggestive of specific biomechanical properties that may influence niche activity as well as mechanotransduction (Daley and Yamada, 2013).

The presence of a distinct GSC niche ECM raised the question of its origin and mechanism of assembly during development. The development of targeted expression of functional GFP-tagged forms of ColIV allowed showing that the GSC niche BM essentially arises from blood cells of the plasmatocyte type that we have called ovarian hemocytes and which contribute to both the regular and interstitial matrices. Ovarian hemocytes originate from the embryo and lymph gland, associate with the larval gonad throughout its development, and then remain associated with the ovaries throughout adulthood. The *Drosophila* plasmatocyte lineage is related to the mammalian myeloid/monocyte lineage, which produces macrophages. Interestingly, resident macrophages have been found to influence the mammary stem cell regenerative response in vertebrates, although the molecular mechanism involved is unknown (reviewed in Wynn et al., 2013). Our findings thus raise the intriguing possibility that macrophages may play a role in controlling the stem cell microenvironment and homeostasis in different organisms.

Our results show that reducing BM levels has dramatic effects on niche organization and homeostasis. Preventing ColIV production by the hemocytes disrupts TF and cap cell organization. Furthermore, the number of stem cells is increased, mimicking a Dpp/BMP gain-of-function phenotype; indeed, increased spreading of Dpp signaling was observed when ColIV levels were affected, a phenotype that can be rescued upon removing

(F) HmlΔ-RFP; He > GFP female gonad (47 hr APF). He > GFP-positive and HmlΔ-RFP-negative cells are detected around the developing germaria along with double-positive cells (arrow). High magnification of the boxed He > GFP HmlΔ-RFP double-positive cell reveals that it is individualized within the gonad and has a morphology similar to differentiated hemocytes.
(G) Cg-GFP gonad (47 hr APF) stained for En (red). Each developing germarium is contacting a Cg-GFP hemocyte (arrows). High magnification of the box reveals that the Cg-GFP hemocyte morphology is comparable to the He > GFP HmlΔ-RFP double-positive cell in (E).
(H) Schematic of the sources of ColIV contributing to the gonad, from larval to adult stages.

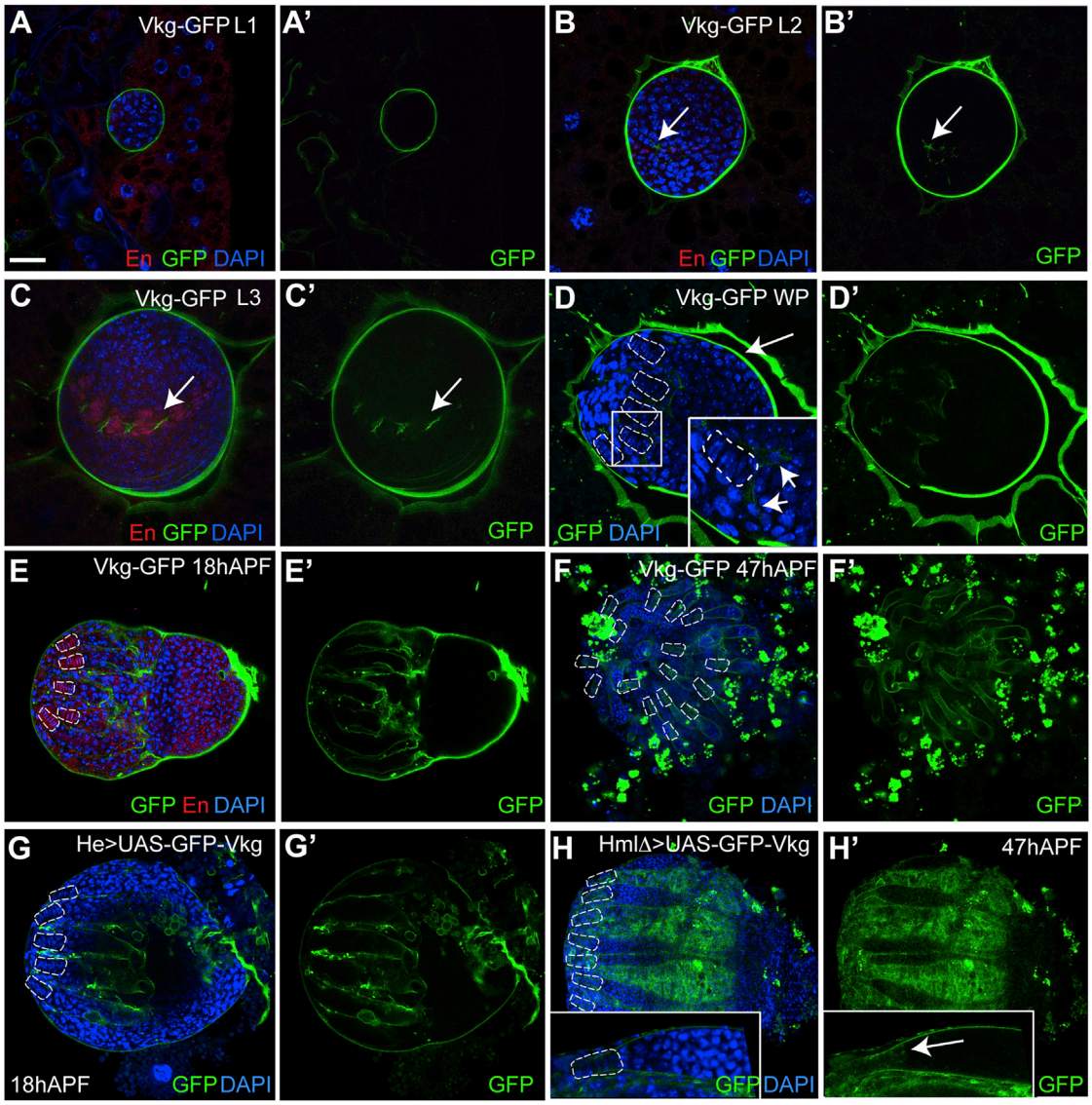

Figure 5. ColIV Deposition in the Developing Female Gonad

(A–C) Vkg-GFP gonad of first (A), second (B), and third (C) instar larvae, stained for DNA (DAPI, blue) and En (red). GFP is found around the gonad at all stages but detected inside the gonad from the second larval instar onward.

(D and D') Vkg-GFP white pupae (WP) gonad surrounded by fat body shows GFP around the TFs (dashed lines; arrowheads in high-magnification box) and in a thick layer around the gonad (arrow). High magnification (box in D) shows that the GFP signal (arrows) is present at the base of the TF (dashed lines).

(E and E') Vkg-GFP gonad (18 hr APF) stained for En (TF, red) and DNA (DAPI, blue). GFP is detected around the gonad and in thin layers surrounding developing germarium (dashed lines in E, TF).

(F and F') Vkg-GFP gonad (47 hr APF) stained for DNA (DAPI, blue). The BM around the gonad is absent. The developing germaria are encapsulated by Vkg-GFP (dashed lines, TF). The GFP debris corresponds to histolysis of fat body.

(G–H') He > UAS-GFP-Vkg (G and G') and HmlΔ > UAS-GFP-Vkg gonad (47 hr APF; H-H'), stained for DNA (DAPI, blue). GFP signal is comparable to (E'). High magnifications of the boxes in (H) and (H') is shown. inGFP-Vkg is incorporated in the BM and in the interstitial matrix embedding the germline stem cell niche (arrow in H').

The scale bar represents 20 μm.

one allele of Dpp. We propose that ColIV is an essential component of the GSC niche microenvironment, necessary to shape the Dpp gradient. Interestingly, in vitro experiments have demonstrated a direct interaction between Dpp and the C-terminal region of Vkg (Wang et al., 2008). Based on these and our data, we propose that Vkg regulates Dpp gradient formation in the ovarian GSC niche through direct protein-protein interaction. Embryonic plasmatocytes have been shown to produce ColIV essential for Dpp signaling and renal tubule formation (Bunt et al., 2010). Therefore, the ability of hemocyte-derived ColIV

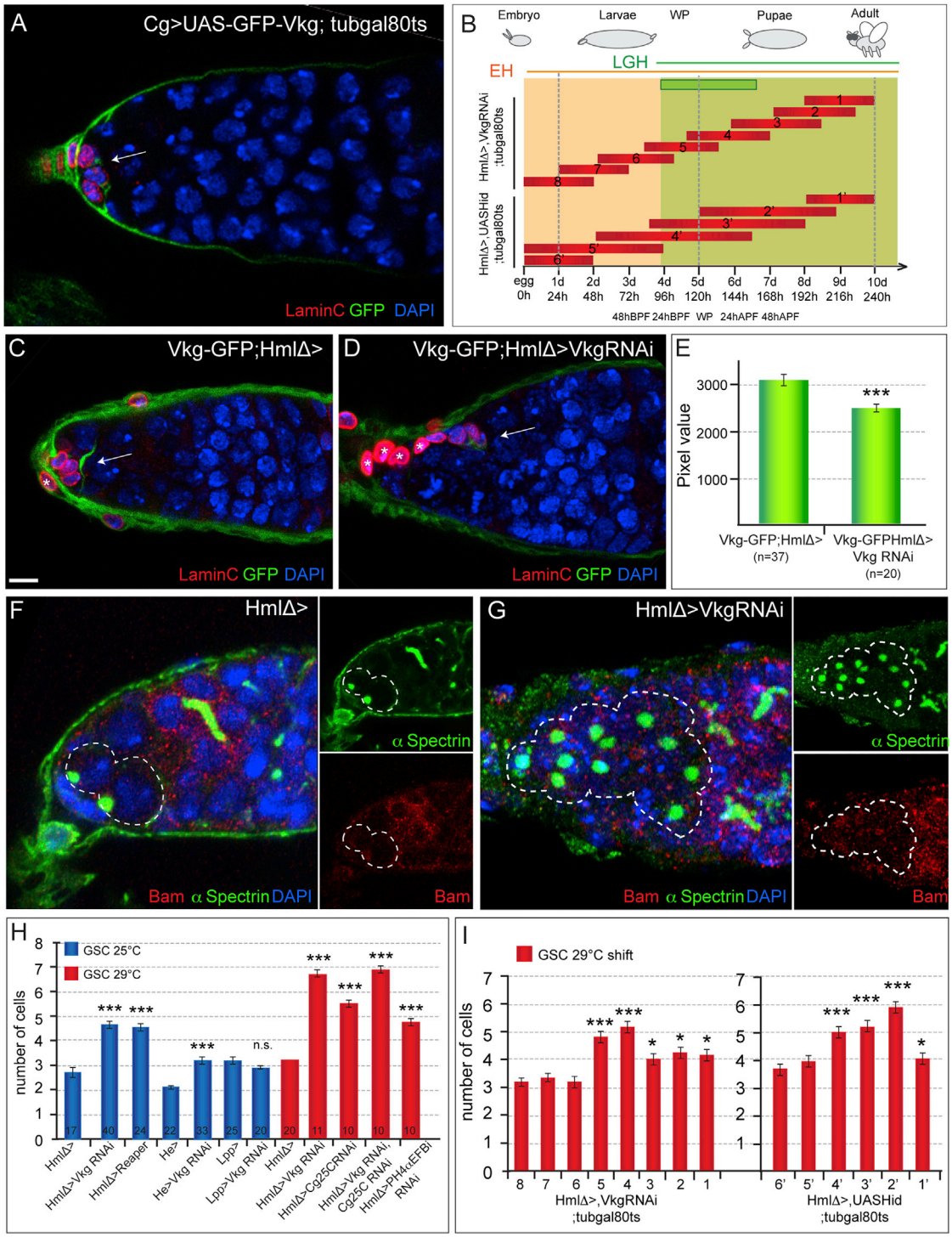

Figure 6. Hemocyte-Produced CollV Regulates Germline Stem Cell Niche Organization and Homeostasis

(A) Cg > UAS-GFP-Vkg; tubGal80ts germarium in which induction of inGFP-Vkg was allowed for 48 hr from 96 hr (see B).

(B) Vkg-RNAi and UAS-Hid expression pulses (in red; numbered 1–8 and 1'–6', respectively). In green, period during which pulses of inGFP-Vkg expression allowed deposition of CollV within the adult germline stem cell niche is shown.

(C and D) Control (Vkg-GFP; HmlΔ >) (C) and Vkg-GFP; HmlΔ > Vkg-RNAi germaria (D) stained for LaminC (red; CpC and TFs) and DNA (DAPI, blue). Asterisks label TF. Arrow highlights the interstitial matrix around the germline stem cell niche. Note the weaker GFP signal in the interstitial matrix and the misorganization of TF and CpC in the Vkg-GFP; HmlΔ > Vkg-RNAi germarium.

(legend continued on next page)

to interact with Dpp and regulate its gradient could be a general mechanism important for morphogenesis.

Multiple Origins of ColIV—an Emerging General Model of BM Assembly

Although the core components of BMs are well conserved and characterized, their mechanism of assembly into mature BM, their diversity, and their origin remain poorly characterized. Current knowledge from flies shows that ColIV originates from diverse sources during development: plasmatocytes in embryos (Bunt et al., 2010; Fessler and Fessler, 1989); fat body in the larvae (Pastor-Pareja and Xu, 2011); and follicle cells in the adult ovary (Denef et al., 2008; Lerner et al., 2013; Medioni and Noselli, 2005). But what remained unclear was the behavior of the newly synthesized ColIV from these sources and whether any specific targeting mechanism existed. In this study, using tissue-specific expression of GFP-tagged forms of ColIV and in situ hybridization, we reveal that not all cell types produce ColIV in ovaries: follicle cells express an essentially cell-autonomous ColIV with no diffusion to other cells, whereas the germarium itself and the muscles do not express BM components. Although being closely associated, neither follicle cells nor muscles contribute to germarium BMs. Instead, we found that companion hemocytes provide most of the niche BM without contributing much to other parts of the adult ovary. Therefore, there is a complex spatially and temporally regulated mechanism of BM deposition in the ovary (and possibly in other organs), with both cell-autonomous and non-autonomous modes of production and assembly.

These observations argue against a single origin for BMs. Instead, our results altogether reveal an interesting mechanism involving specific ''donor'' and ''acceptor'' cells responsible for building the BM of individual organs. This donor-acceptor combination can be cell autonomous (e.g., follicle cells; donor = acceptor) or cell non-autonomous (donor = ovarian hemocytes and acceptor = GSC niche). Furthermore, an acceptor tissue could have one or several donors. For example, although the hemocytes contribute to a stable GSC niche BM, our results also show that the adult fat body contributes to BM in the ovary. Whether these different BMs have the same composition/properties or fulfill different functions (e.g., structural versus maintenance) remains to be established as is the level of BM diversity observed in vivo. Future work using our UAS-GFP-Vkg and UAS-GFP-Cg25c constructs will address this question by establishing an exhaustive atlas of donor-acceptor combinations during *Drosophila* development.

The donor-acceptor model provides an interesting framework to address BM function at the organismal level by proposing the existence of short- and long-range interactions between specific and apparently unrelated cells/organs. An interesting speculation is that the composition and/or nature of an acceptor organ BM could be regulated by the activity/physiology of the donor(s), therefore connecting up tissues and integrating multiple physiological signals into BMs. For instance, because hemocytes are immune cells, they may establish a link between the immune history of the larvae and the adult GSC niche BM properties. Thus, the niche BM could serve as integrator of the larval physiological status and influence the future adult reproductive fitness and/or aging. This imprinting hypothesis is further supported by our finding that the GSC niche BM is highly stable, persisting throughout adult lifespan (more than 60 days).

Another prediction of the model is that specific targeting mechanisms may exist to control deposition of BM components to the appropriate site. Target tissue recognition could involve the expression of specific receptors at the surface of acceptor cells, protein modifications in donor cells making distinct ColIV molecular forms with specific signatures, or any other alternative mechanism.

In conclusion, studying the origin of ovarian ECM allows us to propose a general model of BM assembly in a developing organism. This model reveals emerging properties in BMs, which (1) are diverse in their composition and origin, hence their biochemical traits; (2) originate from specific donor-acceptor combinations; and (3) are imprinted by their temporal and spatial origins. Future work using the versatile *Drosophila* model will provide insights into the mechanisms regulating the diversity and assembly of specific tissue microenvironments and how these translate into normal development, physiology, and disease state.

EXPERIMENTAL PROCEDURES

Fly Strains

Flies were raised on standard medium at 25°C. The following strains were used: Vkg-GFP (vkg^{G454}; Morin et al., 2001); Cg-GFP (Sorrentino et al., 2007); HmlΔGal4 UAS-eGFP; HmlΔ-RFP (P{Hml-dsRed.Δ}; Clark et al., 2011); HeGFP; UASHid;tubGal80ts; He-Gal4 and He-Gal4; UAS-nlsGFP; Dot-Gal4; Cg-Gal4; Lpp-Gal4; Lsp2-Gal4; UAS-Vkg-RNAi (VDRC no. 111668 KK); UAS-Vkg-RNAi; tubGal80ts; UAS-PH4αEFBi-RNAi (TRIP no. HMS00835); UAS-Cg25C-RNAi (VDRC no. 12784); UAS-GFP-Vkg; UAS-GFP-Cg25c; UAS-Reaper; hsFlp; actin > CD2 > Gal4,UAS-GFP; and Dad-lacZ, Dpp^{12}. Unless otherwise specified, 2-day-old flies were analyzed.

Immunohistochemistry

For immunohistochemistry, ovaries were fixed in 1× PBS 3.7% formaldehyde and blocked in 1× PBS, 0.3% Triton X-100, and 2% BSA for 30 min prior to antibodies incubation. To label the BM components, ovaries were fixed in 1× PBS 3.7% formaldehyde 1% DMSO washed three times in 1× PBS, incubated 1 hr in 9:1 MetOH:DMSO at −20°C, and rehydrated in 7:3; 5:5; 3:7 MetOH:PBT (1× PBS Triton 0.1%) three times (5 min). Ovaries were washed three

(E) Quantification of GFP in Vkg-GFP; HmlΔ > and Vkg-GFP; HmlΔ > Vkg-RNAi interstitial matrix. n, number of germaria analyzed. Error bars indicate SEM. *p < 0.05; **p < 0.01; ***p < 0.005 t test versus control.

(F) HmlΔ > germarium stained for bag-of-marbles (Bam, red) and α-spectrin (green) to reveal the GSCs and DNA (DAPI, blue). Two GSC (dashed lines) are recognizable by the presence of a spectrin-positive round spectrosome and the absence of Bam staining.

(G) HmlΔ > Vkg-RNAi germarium containing 11 GSC (dashed lines).

(H) Mean number of GSC per germarium. Blue represents experiments conducted at 25°C; red represents experiments performed at 29°C. Error bars indicate SEM. n.s., non-significant. Controls correspond to Gal4 drivers only. *p < 0.05; **p < 0.01; ***,p < 0.005 t test versus control.

(I) Mean number of GSC per germarium for each Vkg-RNAi and UAS-Hid experiment presented in (B).

The scale bar represents 5 μm. See also Figure S6.

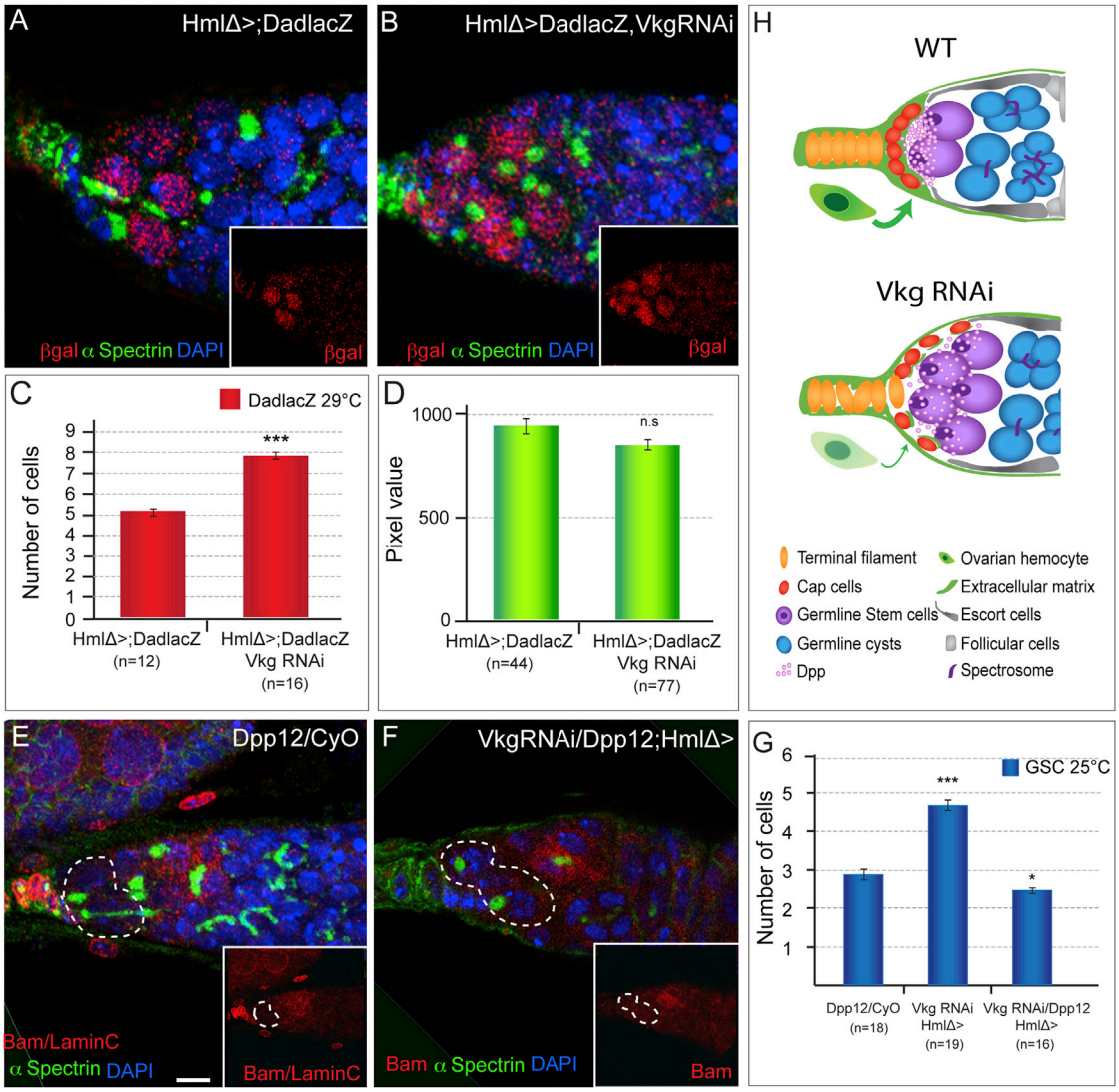

Figure 7. CollV Is Important for Dpp Signaling and Stem Cell Number

(A and B) HmlΔ > ;Dad-lacZ (A) and a HmlΔ > Dad-lacZ,Vkg-RNAi (B) germaria stained for β-galactosidase (β-gal, red), α-spectrin (green) to identify the GSCs, and DNA (DAPI, blue).

(C) Mean number of Dad-lacZ-positive GSC per germarium. Error bars: SEM. *p < 0.05; **p < 0.01; ***p < 0.005 t test versus control. The scale bar represents 5 μm.

(D) Intensity of β-gal in Dad-lacZ-positive GSC. n, number of measurement; n.s., non-significant t test versus control. Error bars represent SEM.

(E and F) Dpp12/CyO and Vkg-RNAi/Dpp12; HmlΔ > germaria stained for BAM, LaminC (red), α-spectrin (green), and DNA (DAPI, blue). Dpp12/CyO (E) germarium contains two GSCs (dashed lines). Vkg-RNAi/Dpp12; HmlΔ > (F) germarium shows a normal number of GSCs (compare with B).

(G) Mean of GSC per germarium. Error bars: SEM. *p < 0.05; **p < 0.01; ***p < 0.005 t test versus control. The scale bar represents 5 μm.

times in PBT and blocked in 1× PBS 0.3% Triton X-100 2% BSA for 2 hr prior to antibodies incubation. Primary antibodies used were mouse anti-Hemese (1:100), mouse anti-Nimrod C1 (anti-P1; 1:30), mouse anti-Atilla (L1; 1:100), and mouse anti-C4 (1:10), all gifts from I. Ando; rabbit anti-GFP N-term (1:20) Sigma; rabbit anti-perlecan (1:2,000; gift from S. Baumgartner); mouse anti-LaminC LC28.26 (DSHB; 1:200), mouse anti-Bam (Bag-of-marbles; 1:100; DSHB); rabbit anti-alpha spectrin (1:200 gift from J.-R. Huynh); rabbit anti-Engrailed (1:200; Santa Cruz); rabbit anti-lamininA (1:3,000; gift from S. Baumgartner); mouse anti-Mys (1:100; DSHB CF.6G11); and rabbit anti-Cg25c (1:500), this paper. Chicken anti-Bgal (1/5,000; Genetex). Secondary antibodies were Alexa Fluor 546, Alexa 488, and Cy5 (Molecular Probes; Jackson ImmunoResearch). Imaging was performed on a confocal microscope Zeiss LSM 780.

Antibody Production

Polyclonal antibodies were raised against Cg25c using the Eurogentec DoubleX protocol. The following peptides were used for rabbit immunization: 37–51 DSVKHYNRNEPKFPI and 751–765 CALDEIKMPAKGNKG.

Fluorescent In Situ Hybridization

Vkg and Cg25c RNA probes were used. Samples were fixed in 1× PBS 3.7% formaldehyde for 10 min, rinsed twice in PBT (1× PBS 0.1% Tween20), pre-hybridized 10 min in 1:1 Hydridation Solution (Hyb):PBT (Hyb: 50% deionized formamide, 5× SSC, 0.1% Tween 20, 50 μg/ml heparin, and 100 μg/ml Hareng Sperm DNA) and 1 hr in Hyb at 65°C. Hybridation was carried out overnight at 65°C. After three washes of 20 min in Hyb and one wash in 1:1

Hyb:PBTw (1× PBS Tween 20 0.1%) at 65°C, samples were washed three times at room temperature (RT) in PBTw, blocked 30 min in PBTw BSA 2%, and incubated with anti-digoxigenin (1:1,000) and anti-GFP N-term (1:20) Sigma at RT. Samples were washed three times for 20 min in PBTw and incubated with secondary antibody (1:500; Jackson ImmunoResearch) before proceeding with the TSA-based detection of *viking* and *cg25C* mRNA.

G-trace

HmlΔGal4xTubGal80ts,UAS-FLP,UbiFRTStopFRTnlsEGFP flies were raised at 18°C and heat shock at 29°C for 48 hr at different developmental stages. At 18°C (restrictive temperature), the Gal4 is inactive and, at 29°C (permissive temperature), the Gal4 is active, triggering the permanent expression of GFP. Control flies were raised constantly at 18°C and 29°C. Results of the experiments are presented as a percentage relative to the control flies raised at 29°C.

Cloning

The GFP insertion site of the Vkg-GFP flies was determined by sequencing, and the same insertion was used for the UAS-GFP-Viking. For UAS-GFP-Viking and UAS-GFP-Cg25C transgenic lines, the full-length coding sequence of Viking or Cg25c in which the GFP was inserted after nucleotide 94 for Viking and after nucleotide 78 for Cg25c were cloned in pUAST-C5 (EcoRI-NheI). Full-length constructs (6,587 nt for Vkg [NM_001273142.1] and 6,116 nt for Cg25c [NM_164615]) were synthesized (Epoch Life Science), allowing a GFP fusion without the insertion of additional restriction site or amino acids.

TEM

Ovaries were fixed for 1 hr at RT (1.5% glutaraldehyde in 0.075 M cacodylate buffer). After embedding in resin (Epon mix), longitudinal ovaries ultrathin sections were prepared. Sections were stained in uranyl acetate and lead citrate. Ultrathin sections were observed with a Phillips CM120 electron microscope equipped with a Gatan digital CCD camera at the Centre Technologique des Microstructures (UCBL), Lyon Bio-image platform.

SUPPLEMENTAL INFORMATION

Supplemental Information includes Supplemental Experimental Procedures, four figures, and one movie and can be found with this article online at http://dx.doi.org/10.1016/j.celrep.2015.09.008.

AUTHOR CONTRIBUTIONS

V.V.D.B., G.Z., L.P., D.C., M.M., and T.J. conducted the experiments; V.V.D.B., F.R., and S.N. designed the experiments; and V.V.D.B. and S.N. wrote the manuscript.

ACKNOWLEDGMENTS

We thank Jean-René Huynh, S. Baumgartner, H. Ashe, and I. Ando for reagents and stocks and R. Delanoue and C. Geminard for critical reading of the manuscript. Work in S.N. laboratory is supported by the "Centre National de la Recherche Scientifique," the "Ministère de la Recherche et de l'Enseignement Supérieur," the "Agence Nationale de la Recherche" (program ANR-09-BLAN-0113), the "Association Française contre les Myopathies," and LABEX SIGNALIFE (no. ANR-11-LABX-0028-01).

Received: March 2, 2015
Revised: April 27, 2015
Accepted: September 1, 2015
Published: October 8, 2015

REFERENCES

Asha, H., Nagy, I., Kovacs, G., Stetson, D., Ando, I., and Dearolf, C.R. (2003). Analysis of Ras-induced overproliferation in Drosophila hemocytes. Genetics *163*, 203–215.

Bateman, J.F., Boot-Handford, R.P., and Lamandé, S.R. (2009). Genetic diseases of connective tissues: cellular and extracellular effects of ECM mutations. Nat. Rev. Genet. *10*, 173–183.

Blumberg, B., MacKrell, A.J., and Fessler, J.H. (1988). Drosophila basement membrane procollagen alpha 1(IV). II. Complete cDNA sequence, genomic structure, and general implications for supramolecular assemblies. J. Biol. Chem. *263*, 18328–18337.

Bunt, S., Hooley, C., Hu, N., Scahill, C., Weavers, H., and Skaer, H. (2010). Hemocyte-secreted type IV collagen enhances BMP signaling to guide renal tubule morphogenesis in Drosophila. Dev. Cell *19*, 296–306.

Casanueva, M.O., and Ferguson, E.L. (2004). Germline stem cell number in the Drosophila ovary is regulated by redundant mechanisms that control Dpp signaling. Development *131*, 1881–1890.

Chen, D., and McKearin, D. (2003). Dpp signaling silences bam transcription directly to establish asymmetric divisions of germline stem cells. Curr. Biol. *13*, 1786–1791.

Clark, R.I., Woodcock, K.J., Geissmann, F., Trouillet, C., and Dionne, M.S. (2011). Multiple TGF-β superfamily signals modulate the adult Drosophila immune response. Curr. Biol. *21*, 1672–1677.

Daley, W.P., and Yamada, K.M. (2013). ECM-modulated cellular dynamics as a driving force for tissue morphogenesis. Curr. Opin. Genet. Dev. *23*, 408–414.

Daley, W.P., Peters, S.B., and Larsen, M. (2008). Extracellular matrix dynamics in development and regenerative medicine. J. Cell Sci. *121*, 255–264.

Denef, N., Chen, Y., Weeks, S.D., Barcelo, G., and Schüpbach, T. (2008). Crag regulates epithelial architecture and polarized deposition of basement membrane proteins in Drosophila. Dev. Cell *14*, 354–364.

Devergne, O., Tsung, K., Barcelo, G., and Schüpbach, T. (2014). Polarized deposition of basement membrane proteins depends on Phosphatidylinositol synthase and the levels of Phosphatidylinositol 4,5-bisphosphate. Proc. Natl. Acad. Sci. USA *111*, 7689–7694.

Evans, C.J., Olson, J.M., Ngo, K.T., Kim, E., Lee, N.E., Kuoy, E., Patananan, A.N., Sitz, D., Tran, P., Do, M.-T., et al. (2009). G-TRACE: rapid Gal4-based cell lineage analysis in *Drosophila*. Nature Methods *6*, 603–605.

Fessler, J.H., and Fessler, L.I. (1989). Drosophila extracellular matrix. Annu. Rev. Cell Biol. *5*, 309–339.

Gattazzo, F., Urciuolo, A., and Bonaldo, P. (2014). Extracellular matrix: a dynamic microenvironment for stem cell niche. Biochim. Biophys. Acta *1840*, 2506–2519.

Gold, K.S., and Brückner, K. (2014). Drosophila as a model for the two myeloid blood cell systems in vertebrates. Exp. Hematol. *42*, 717–727.

Grigorian, M., Mandal, L., and Hartenstein, V. (2011). Hematopoiesis at the onset of metamorphosis: terminal differentiation and dissociation of the Drosophila lymph gland. Dev. Genes Evol. *221*, 121–131.

Guo, Z., and Wang, Z. (2009). The glypican Dally is required in the niche for the maintenance of germline stem cells and short-range BMP signaling in the Drosophila ovary. Development *136*, 3627–3635.

Haigo, S.L., and Bilder, D. (2011). Global tissue revolutions in a morphogenetic movement controlling elongation. Science *331*, 1071–1074.

Harris, R.E., and Ashe, H.L. (2011). Cease and desist: modulating short-range Dpp signalling in the stem-cell niche. EMBO Rep. *12*, 519–526.

Holz, A., Bossinger, B., Strasser, T., Janning, W., and Klapper, R. (2003). The two origins of hemocytes in Drosophila. Development *130*, 4955–4962.

Horne-Badovinac, S., Hill, J., Gerlach, G., 2nd, Menegas, W., and Bilder, D. (2012). A screen for round egg mutants in Drosophila identifies tricornered, furry, and misshapen as regulators of egg chamber elongation. G3 (Bethesda) *2*, 371–378.

Hudson, A.M., Petrella, L.N., Tanaka, A.J., and Cooley, L. (2008). Mononuclear muscle cells in Drosophila ovaries revealed by GFP protein traps. Dev. Biol. *314*, 329–340.

Jung, S.H., Evans, C.J., Uemura, C., and Banerjee, U. (2005). The Drosophila lymph gland as a developmental model of hematopoiesis. Development *132*, 2521–2533.

Khoshnoodi, J., Pedchenko, V., and Hudson, B.G. (2008). Mammalian collagen IV. Microsc. Res. Tech. *71*, 357–370.

Kim, S.H., Turnbull, J., and Guimond, S. (2011). Extracellular matrix and cell signalling: the dynamic cooperation of integrin, proteoglycan and growth factor receptor. J. Endocrinol. *209*, 139–151.

Krzemien, J., Oyallon, J., Crozatier, M., and Vincent, A. (2010). Hematopoietic progenitors and hemocyte lineages in the Drosophila lymph gland. Dev. Biol. *346*, 310–319.

Kurucz, E., Zettervall, C.J., Sinka, R., Vilmos, P., Pivarcsi, A., Ekengren, S., Hegedüs, Z., Ando, I., and Hultmark, D. (2003). Hemese, a hemocyte-specific transmembrane protein, affects the cellular immune response in Drosophila. Proc. Natl. Acad. Sci. USA *100*, 2622–2627.

Lanot, R., Zachary, D., Holder, F., and Meister, M. (2001). Postembryonic hematopoiesis in Drosophila. Dev. Biol. *230*, 243–257.

Lebestky, T., Chang, T., Hartenstein, V., and Banerjee, U. (2000). Specification of Drosophila hematopoietic lineage by conserved transcription factors. Science *288*, 146–149.

LeBleu, V.S., Macdonald, B., and Kalluri, R. (2007). Structure and function of basement membranes. Exp. Biol. Med. (Maywood) *232*, 1121–1129.

Lerner, D.W., McCoy, D., Isabella, A.J., Mahowald, A.P., Gerlach, G.F., Chaudhry, T.A., and Horne-Badovinac, S. (2013). A Rab10-dependent mechanism for polarized basement membrane secretion during organ morphogenesis. Dev. Cell *24*, 159–168.

Losick, V.P., Morris, L.X., Fox, D.T., and Spradling, A. (2011). Drosophila stem cell niches: a decade of discovery suggests a unified view of stem cell regulation. Dev. Cell *21*, 159–171.

Lu, P., Weaver, V.M., and Werb, Z. (2012). The extracellular matrix: a dynamic niche in cancer progression. J. Cell Biol. *196*, 395–406.

Lunstrum, G.P., Bächinger, H.P., Fessler, L.I., Duncan, K.G., Nelson, R.E., and Fessler, J.H. (1988). Drosophila basement membrane procollagen IV. I. Protein characterization and distribution. J. Biol. Chem. *263*, 18318–18327.

Makhijani, K., and Brückner, K. (2012). Of blood cells and the nervous system: hematopoiesis in the Drosophila larva. Fly (Austin) *6*, 254–260.

Makhijani, K., Alexander, B., Tanaka, T., Rulifson, E., and Brückner, K. (2011). The peripheral nervous system supports blood cell homing and survival in the Drosophila larva. Development *138*, 5379–5391.

Medioni, C., and Noselli, S. (2005). Dynamics of the basement membrane in invasive epithelial clusters in Drosophila. Development *132*, 3069–3077.

Morin, X., Daneman, R., Zavortink, M., and Chia, W. (2001). A protein trap strategy to detect GFP-tagged proteins expressed from their endogenous loci in Drosophila. Proc. Natl. Acad. Sci. USA *98*, 15050–15055.

Pastor-Pareja, J.C., and Xu, T. (2011). Shaping cells and organs in Drosophila by opposing roles of fat body-secreted Collagen IV and perlecan. Dev. Cell *21*, 245–256.

Ricard-Blum, S., and Ruggiero, F. (2005). The collagen superfamily: from the extracellular matrix to the cell membrane. Pathol. Biol. (Paris) *53*, 430–442.

Sahut-Barnola, I., Godt, D., Laski, F.A., and Couderc, J.L. (1995). Drosophila ovary morphogenesis: analysis of terminal filament formation and identification of a gene required for this process. Dev. Biol. *170*, 127–135.

Schofield, R. (1978). The relationship between the spleen colony-forming cell and the haemopoietic stem cell. Blood Cells *4*, 7–25.

Song, X., Zhu, C.H., Doan, C., and Xie, T. (2002). Germline stem cells anchored by adherens junctions in the Drosophila ovary niches. Science *296*, 1855–1857.

Song, X., Wong, M.D., Kawase, E., Xi, R., Ding, B.C., McCarthy, J.J., and Xie, T. (2004). Bmp signals from niche cells directly repress transcription of a differentiation-promoting gene, bag of marbles, in germline stem cells in the Drosophila ovary. Development *131*, 1353–1364.

Sorrentino, R.P., Tokusumi, T., and Schulz, R.A. (2007). The Friend of GATA protein U-shaped functions as a hematopoietic tumor suppressor in Drosophila. Dev. Biol. *311*, 311–323.

Spradling, A., Drummond-Barbosa, D., and Kai, T. (2001). Stem cells find their niche. Nature *414*, 98–104.

Tanimura, S., Tadokoro, Y., Inomata, K., Binh, N.T., Nishie, W., Yamazaki, S., Nakauchi, H., Tanaka, Y., McMillan, J.R., Sawamura, D., et al. (2011). Hair follicle stem cells provide a functional niche for melanocyte stem cells. Cell Stem Cell *8*, 177–187.

Tepass, U., Fessler, L.I., Aziz, A., and Hartenstein, V. (1994). Embryonic origin of hemocytes and their relationship to cell death in Drosophila. Development *120*, 1829–1837.

Wang, X., Harris, R.E., Bayston, L.J., and Ashe, H.L. (2008). Type IV collagens regulate BMP signalling in Drosophila. Nature *455*, 72–77.

Watt, F.M., and Huck, W.T. (2013). Role of the extracellular matrix in regulating stem cell fate. Nat. Rev. Mol. Cell Biol. *14*, 467–473.

Wong, V.W., Levi, B., Rajadas, J., Longaker, M.T., and Gurtner, G.C. (2012). Stem cell niches for skin regeneration. Int. J. Biomater. *2012*, 926059.

Wood, W., and Jacinto, A. (2007). Drosophila melanogaster embryonic haemocytes: masters of multitasking. Nat. Rev. Mol. Cell Biol. *8*, 542–551.

Wynn, T.A., Chawla, A., and Pollard, J.W. (2013). Macrophage biology in development, homeostasis and disease. Nature *496*, 445–455.

Xie, T., and Spradling, A.C. (1998). decapentaplegic is essential for the maintenance and division of germline stem cells in the Drosophila ovary. Cell *94*, 251–260.

Yurchenco, P.D. (2011). Basement membranes: cell scaffoldings and signaling platforms. Cold Spring Harb. Perspect. Biol. *3*, pii: a004911.